# Decoding the Geodynamo: Quantitative Dependence of Magnetic Field Diagnostics on Dimensionless Control Parameters

*Klaudio* Peqini[1], *Ilirjan* Margjeka[2], *Rudina* Osmanaj[1], *Enkelejd* Çaça[3], *Olta* Çakaj[1]

[1]Department of Physics, Faculty of Natural Sciences, University of Tirana, Blvd. Zogu I, No. 25, 1001, Tirane, Albania
[2]Istituto Nazionale di Fisica Nucleare, Sezzione Bari, Bari, Italy, on leave
[3]Department of Physics Engineering, Faculty of Mathematical Engineering and Physics Engineering, Polytechnic University of Tirana, Sq. Mother Teresa, Tirane, Albania
e-mail: klaudio.peqini@fshn.edu.al

**Abstract.** Understanding how planetary magnetic fields are generated and sustained requires careful analysis of how key physical quantities respond to changes in the underlying control parameters. In this work, we focus on the scaling behaviour of magnetic energy, dipolarity, field symmetry, and temporal variability with respect to the Rayleigh number (Ra), a key driver of convective vigour. Using the XSHELLS simulation framework, we carry out a series of dynamo simulations in rotating spherical shells, systematically varying Ra along with the Ekman number (E) and magnetic Prandtl number (Pm). Our results highlight clear transitions in magnetic field structure—from strong, stable dipoles to weaker, multipolar states—as Ra increases. We identify scaling laws that relate the intensity and geometry of the magnetic field to Ra and Pm, and track how spectral energy distributions shift with these parameters. In particular, we find that decreasing E leads to the development of rotationally constrained flows and quasi-geostrophic dynamics, which strongly influence magnetic field morphology. Overall, this study emphasizes the role of Ra as a central control parameter in dynamo models and provides a clearer picture of how convective forcing shapes planetary magnetic fields.

**Keywords:** Geodynamo, Dimensionless Control Parameters, Ekman Number, Rayleigh Number, Magnetic Prandtl Number, Convection-driven Magnetohydrodynamics

## 1 Introduction

Planetary magnetic fields are the result of dynamo action: a process in which fluid motion in a conducting medium converts kinetic energy into magnetic energy. In the case of Earth, this takes place in the fluid outer core, where thermochemical convection of liquid iron in the presence of planetary rotation gives rise to the geomagnetic field. This field plays a vital role in shielding the planet from solar wind and cosmic radiation, and its long-term behaviour –

including secular variation and polarity reversals – has been a subject of scientific interest for over a century [1–3].

Understanding the mechanisms behind dynamo action remains one of the central challenges in geophysics and planetary science. The governing equations of magnetohydrodynamics (MHD), when applied to a rotating spherical shell under the Boussinesq approximation, provide a theoretical foundation to investigate dynamo processes. Numerical simulations of these equations have been instrumental in advancing our understanding of core dynamics, especially through the identification of various dynamo regimes and force balances [4–8]. However, due to the extreme parameter values characteristic of Earth's core – such as very low Ekman numbers and high Rayleigh numbers – direct numerical simulations at realistic conditions remain computationally inaccessible. This has motivated the development of scaling laws that can relate observable quantities (e.g., magnetic field strength, flow speed, heat transport) to dimensionless control parameters such as the Rayleigh number $Ra$, the Ekman number $E$, and the magnetic Prandtl number $Pm$ [9–12].

Among these parameters, the Rayleigh number plays a particularly important role, as it quantifies the strength of the buoyancy forcing relative to diffusive effects, and thereby controls the vigour of convective motion. In planetary settings, $Ra$ can span many orders of magnitude, and its variation is closely linked to changes in the internal heat budget, core composition, and secular cooling [13–15]. Although extensive efforts have been made to describe how global dynamo quantities such as magnetic energy, dipolarity, or heat flux scale with $Ra$ [16–20], much less attention has been given to the scaling of velocity components individually, especially in spherical coordinates. Yet, such information is essential for understanding the spatial structure of convective flows and their role in the induction process. In particular, radial and azimuthal velocity components have distinct physical implications: the former is associated with heat transport and upwelling/down-welling flows, while the latter is closely linked to zonal winds and large-scale shear.

In this paper, we aim to identify preliminary scaling relationships between the Rayleigh number and the mean values of the velocity components in the spherical coordinate system $(r, \theta, \phi)$. This is achieved through a suite of numerical simulations of convection-driven dynamos in rotating spherical shells, performed over a broad range of Rayleigh numbers while keeping other relevant parameters fixed. Our results contribute to the ongoing effort of building predictive scaling frameworks for planetary dynamos, with implications for both terrestrial and other planetary magnetic fields.

The paper is organized as follows: in section 2 we discuss the model, the numerical environment used to simulate the model and the numerical setup. In section 3 we provide some preliminary results and in section 4 we discuss these findings. The paper ends with some conclusions.

## 2 The model and XSHELLS

### 2.1 The model

The physical model studied in this work is based on the classical approach to simulating convection-driven dynamos in rotating spherical shells. This configuration serves as an idealized yet physically meaningful representation of Earth's outer core and those of other terrestrial planets. The model assumes a spherical shell filled with an electrically conducting, incompressible fluid, subject to an imposed temperature contrast between the inner and outer boundaries, and rotating uniformly around the vertical axis. The flow is driven by buoyancy forces resulting from internal heating or boundary-driven thermal gradients, and it is

influenced by Coriolis forces due to planetary rotation. This setup captures the essential force balances at play in planetary interiors – particularly the interaction between inertial, Coriolis, buoyancy, viscous, and Lorentz forces – while remaining computationally tractable for numerical exploration [21–23].

To make the system more amenable to numerical analysis, we adopt the Boussinesq approximation, which assumes that density variations are negligible except where they appear in the buoyancy term. This simplification allows for energy-conserving formulations and avoids the complexities introduced by compressibility, while still preserving the basic structure of convective motions and their interaction with magnetic fields [24, 25]. The governing equations are non-dimensional using the shell thickness $D = r_o - r_i$ as the length scale, the viscous diffusion time $D^2/\nu$ as the time scale, and the imposed temperature drop $\Delta T$ as the temperature scale. The magnetic field is scaled by $(\rho\mu\eta\Omega)^{1/2}$, yielding the following dimensionless system of equations:

$$\frac{\partial \mathbf{u}}{\partial t} + (\mathbf{u}\cdot\nabla\mathbf{u}) + \frac{2}{E}\hat{\mathbf{z}}\times\mathbf{u} = -\nabla p + \frac{Ra}{Pr}T\mathbf{r} + (\nabla\times\mathbf{B})\times\mathbf{B} + \nabla^2\mathbf{u} \qquad (1)$$

$$\frac{\partial \mathbf{B}}{\partial t} = \nabla\times(\mathbf{u}\times\mathbf{B}) + \nabla^2\mathbf{B} \qquad (2)$$

$$\frac{\partial T}{\partial t} + (\mathbf{u}\cdot\nabla\mathbf{T}) = \nabla^2 T \qquad (3)$$

$$\nabla\cdot\mathbf{u} = 0, \quad \nabla\cdot\mathbf{B} = 0 \qquad (4)$$

Equation (1) is the Navier-Stokes equation for an electrically conducting fluid flow in the presence of viscous forces and governs the evolution of the fluid flow. Equation (2) is the induction equation that describes the dynamics of the magnetic field as the outcome of two competing mechanisms, the generation process due to the interaction with the velocity field (first term on the R.H.S.) and the dissipative process due to magnetic diffusion (second term on R.H.S.). Meanwhile, equation (3) is the heat equation that allows the reconstruction of the temperature field across the outer core. Equations (4) impose the non-compressibility of the fluid flow and allow divergence-less magnetic fields as solutions.

In these equations, **u** is the velocity field, **B** the magnetic field, $T$ the temperature perturbation, and p the modified pressure. The key dimensionless control parameters are: the Rayleigh number $Ra = \alpha g \Delta T D^3/(\nu\kappa)$, which quantifies the strength of buoyancy forcing; the Ekman number $E = \nu/(\Omega D^2)$, which measures the relative importance of viscous to Coriolis forces; the Prandtl number $Pr = \nu/\kappa$, representing the ratio of viscous to thermal diffusivity; and the magnetic Prandtl number $Pm = \nu/\eta$, which characterizes the ratio of viscous to magnetic diffusion. These four parameters determine the dynamical regime of the system and are varied across different studies to explore diverse behaviours, from weak convection to strongly chaotic, turbulent dynamos [26–29]. In this study, we focus on the scaling of the velocity field components with respect to $Ra$, while keeping other parameters fixed, thus isolating the effects of thermal forcing on convective flow structure.

### 2.2 The XSHELLS Framework

In the study of planetary dynamo processes, resolving the wide range of spatial and temporal scales present in convection-driven turbulence remains a major computational challenge. Classical pseudo-spectral codes based on spherical harmonics offer high accuracy but often suffer from poor scalability on modern parallel architectures. This limitation has

led to the development of alternative frameworks that retain spectral accuracy while improving parallel performance. One of the most effective and widely used tools in this context is XSHELLS – a high-performance numerical code designed to solve the magnetohydrodynamic (MHD) equations in rotating spherical shells under the Boussinesq approximation [30]. The code was developed to address the need for scalable simulations of spherical convection and dynamo processes at low Ekman numbers and high Rayleigh numbers, where traditional codes encounter computational bottlenecks.

XSHELLS combines spherical harmonic decomposition in the horizontal directions with finite-difference discretization in the radial direction. This hybrid approach allows for both high accuracy and efficient domain decomposition, which makes the code exceptionally well-suited for massively parallel computations. It uses an implicit-explicit (IMEX) time-stepping scheme, where linear terms (e.g., diffusion, Coriolis force) are treated implicitly while nonlinear terms are handled explicitly. This formulation enables stable integration over long timescales even in highly turbulent regimes. XSHELLS also includes options for stress-free or no-slip mechanical boundary conditions and for fixed temperature or fixed flux thermal boundary conditions, making it adaptable to a wide variety of physical setups [31, 32]. The equations are written in dimensionless form and solved for the velocity, magnetic field, and temperature fields simultaneously, making it ideal for convection-driven dynamo studies.

One of XSHELLS' most notable features is its ability to simulate flows at very low Ekman numbers, down to $E \sim 10^{-7}$ or lower, which is critical for exploring asymptotic geodynamo behaviour. It supports high-resolution simulations with spherical harmonic truncations exceeding $l_{max} = 1000$, and scales efficiently across thousands of CPU cores using MPI-based parallelization. The code has been benchmarked and validated extensively against other numerical dynamo codes and analytical test cases [33]. Its computational performance has enabled long-time integrations over multiple magnetic diffusion times, making it a powerful tool for studying magnetic field reversals, secular variation, and chaotic dynamics.

XSHELLS has already played a central role in several ground-breaking studies. For example, Schaeffer et al. (2017) used it to produce one of the first geodynamo simulations that reach Earth-like force balances (magnetostrophic regime) at moderate magnetic Reynolds numbers [32]. The code has also been used to explore the formation of torsional oscillations, investigate the influence of magnetic boundary conditions, and study scaling behaviour in rapidly rotating convection [34, 35]. More recent applications include modelling core flows constrained by geomagnetic observations [36] and analysing scaling laws in strongly turbulent dynamos [37]. Given its versatility, precision, and performance, XSHELLS represents one of the most advanced and reliable tools currently available for numerical studies of geophysical and planetary dynamos.

### 2.3 Numerical Integration

The numerical simulations presented in this study were carried out using a high-resolution implementation of the Boussinesq MHD equations in a rotating spherical shell, as described in the previous sections. The inner and outer radii of the shell are set to $r_i = 0.35$ and $r_o = 1$, giving an aspect ratio $\chi = r_i/r_o = 0.35$, which is close to that of the Earth's outer core. The velocity field satisfies stress-free boundary conditions at both the inner and outer shells, while temperature is fixed at both boundaries. Magnetic boundary conditions correspond to electrically insulating surroundings. The equations are solved using a pseudo-spectral decomposition in the angular directions and second-order finite differences in the radial direction. Temporal integration is performed using an implicit-explicit (IMEX) scheme. Simulations were carried out with spherical harmonic truncation up to $l_{max} = 171$, and radial resolution of 96 grid points, ensuring spectral convergence for the entire parameter range studied. Simulations with higher Ra require much larger $l_{max}$ and higher radial resolution.

The focus of this study is on understanding how the mean values of the three velocity components – radial ($u_r$), latitudinal ($u_\theta$), and azimuthal ($u_\phi$) – vary as a function of the Rayleigh number $Ra$, which controls the thermal forcing. To isolate the role of convective vigour, all other dimensionless parameters are held constant: the Ekman number is fixed at $E = 10^{-4}$, and the magnetic Prandtl number at $Pm = 1$. The Rayleigh number is varied over in the range 80 to 180. We are aware that the values used in these simulations are far away from the assumed range in the outer core. However, the aim with the actual paper is to show that

Each simulation is evolved over several viscous diffusion times to ensure the system reaches a statistically steady state. Time-averaged quantities are computed from the saturated regime, and spatial averaging is performed over spherical shells to capture large-scale features. The goal is to extract scaling relationships of the form $\langle u_i \rangle \sim Ra^{\alpha}$, where $u_i \in \{u_r, u_\theta, u_\phi\}$, and to interpret the resulting exponents in light of force balances and convection dynamics. In this paper we will not provide such relations, as we are in the initial phases of our project and we will limit ourselves in providing some preliminary results. The scaling laws will be provided in a forthcoming paper that will contain most of the ongoing work.

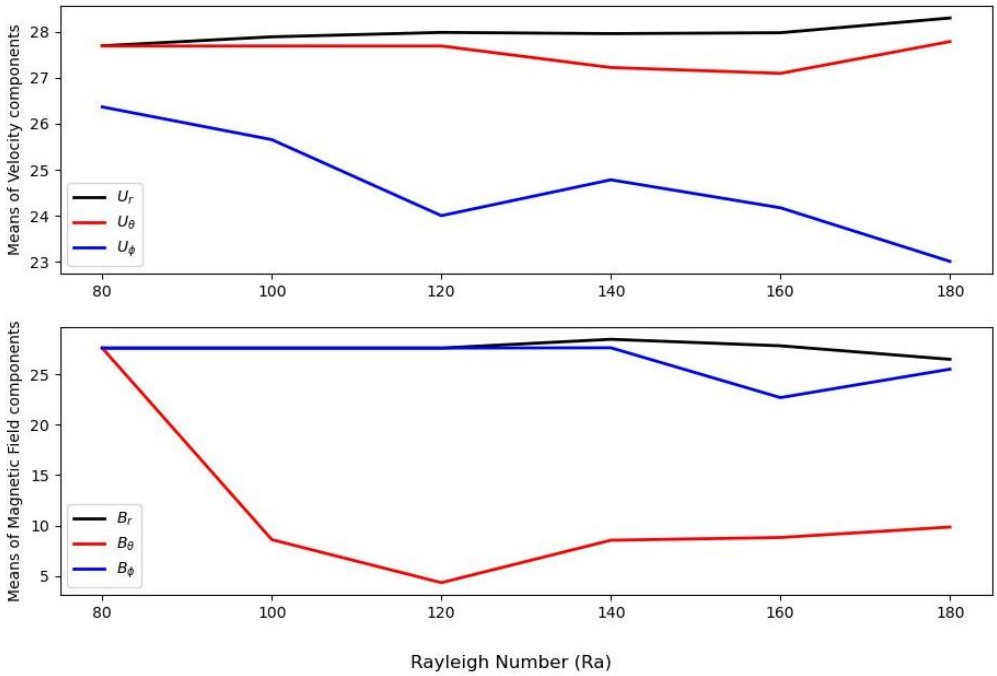


**Fig. 1.** Mean of velocity components $\{u_r, u_\theta, u_\phi\}$ in spherical coordinates, calculated for the spherical shell half way from the inner core boundary to the core-mantle boundary (upper panel). Mean of magnetic field components $\{B_r, B_\theta, B_\phi\}$ in spherical coordinates, calculated for the spherical shell half way from the inner core boundary to the core-mantle boundary (upper panel).

## 3 Results

We have analysed two spherical shells, one half way from the inner core boundary to the core-mantle boundary, and the other very close to the latter. Next, we have calculated the mean of each component for each shell and the results are plotted in Fig. 1 and Fig. 2,

respectively. The limited range of Ra does not allow us to arrive at robust conclusions regarding possible scaling laws and the respective exponents. However, we notice that $u_\phi$ and $B_\theta$ have a considerable decrease, as *Ra* increases. Meanwhile the other components remain virtually unchanged, or vary just slightly. Considering the typical relations of **u** and **B** in the dynamo mechanism, where the toroidal $(0, 0, u_\phi)$ (poloidal $(u_r, u_\theta, 0)$) velocity field is related to the poloidal $(B_r, B_\theta, 0)$ (toroidal $(0, 0, B_\phi)$) magnetic field [2, 6, 16, 21, 22], these graphs are just a manifestation of the terrestrial dynamo in action.

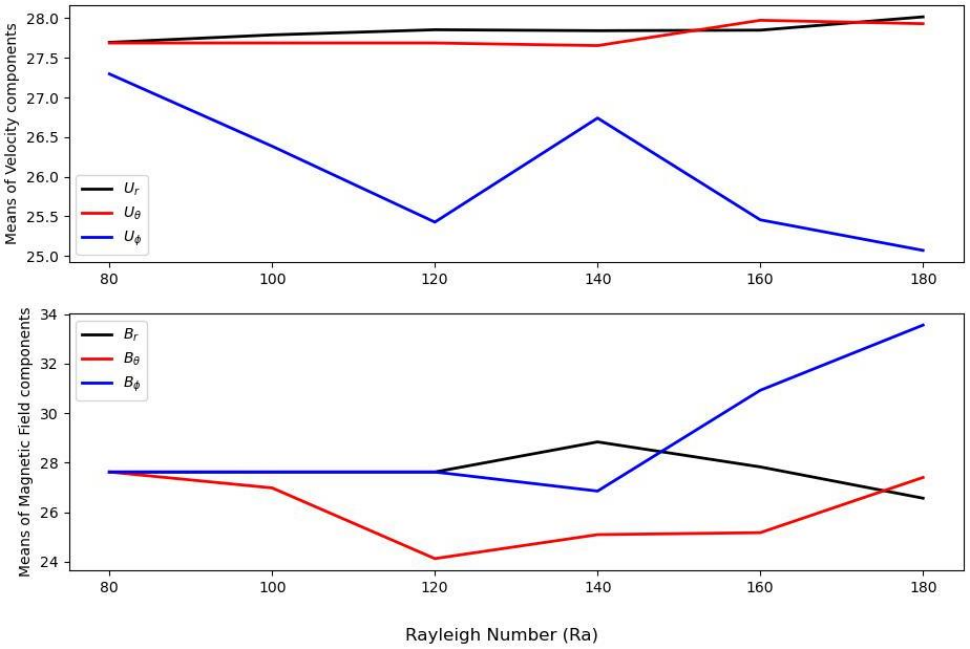


**Fig. 2.** Mean of velocity components $\{u_r, u_\theta, u_\phi\}$ in spherical coordinates, calculated for the spherical shell close to the core-mantle boundary (upper panel). Mean of magnetic field components $\{B_r, B_\theta, B_\phi\}$ in spherical coordinates, calculated for the spherical shell close to the core-mantle boundary (upper panel).

The first shell is in the bulk of the outer core and there the fluid flow is much less affected by boundary layer effects. The mean of the velocity components and the magnetic field components related by the dynamo mechanism vary smoothly and hand-by-hand with each-other. The situation is not so clear in the case of the second shell, where we notice that components have larger variations. We speculate that such rougher variations are due to the nearby core-mantle boundary that are enhanced as *Ra* increases. The fact we can observe such fact within such a limited range of *Ra*, indicates that the geodynamo is an extremely sensitive system.

## 4 Discussion

Convection in Earth's outer core operates in an extreme regime characterized by very low viscosity, strong rotation, and weak stratification. The Ekman number is estimated to be around $E \sim 10^{-15}$, and the Rayleigh number likely exceeds $10^9$, placing the system deep into a rotationally dominated turbulent regime [32]. Under such conditions, convection is strongly anisotropic: fluid motions are organized into columnar structures aligned with the rotation

axis (Taylor columns), and the flow is largely quasi-geostrophic, meaning that the Coriolis force nearly balances the pressure gradient [33]. These constraints lead to flow patterns that differ substantially from classical Rayleigh–Bénard convection and require specialized modelling approaches that respect rotational symmetry and scale separation. Simulations using intermediate Ekman numbers, such as those in this study, provide valuable insights into how flow and field morphologies evolve as one transitions toward more realistic planetary regimes.

A central aspect of outer core convection is the transport of energy – primarily thermal or compositional – from the inner core boundary to the outer core-mantle boundary. In numerical models, this is often analysed through the Nusselt number or, indirectly, through the amplitudes and structure of the convective velocities. The radial component of velocity ($u_r$) governs vertical heat transport, while the azimuthal component ($u_\phi$) often reflects the presence of zonal flows and geostrophic balance. The latitudinal component ($u_\theta$) captures secondary flows driven by the interaction of rotation and buoyancy. These components can exhibit different scaling behaviours depending on the dominance of Coriolis, Lorentz, and buoyancy forces. For example, in magnetostrophic balance – thought to apply in the Earth's core – the Lorentz and Coriolis forces play a dominant role, constraining the amplitudes and spatial profiles of the velocity and magnetic fields [34–36]. The analysis of these individual components, as performed in this study, helps to illuminate the structure of the flow and its role in sustaining the geodynamo.

The results of our simulations broadly align with previous studies of convection-driven dynamos in rotating spherical shells. For instance, studies by King & Soderlund [38] and Soderlund [39] have shown that as $Ra$ increases, flow velocities do not necessarily grow uniformly across all components. Instead, different components exhibit different sensitivities to buoyancy forcing due to anisotropies introduced by rapid rotation and magnetic feedback. Our findings reinforce this picture: while $u_r$ and $u_\theta$ exhibit relatively stable trends with moderate variation, the azimuthal velocity component $u_\phi$, often associated with large-scale zonal flow, shows non-monotonic behaviour. This agrees with earlier results indicating that zonal flows may be inhibited or enhanced depending on the dynamical regime [40]. The mean magnetic field components also reflect the evolving force balances; in particular, the relative growth of $B_\phi$ at higher $Ra$, especially close to the core-mantle boundary, supports the idea that the toroidal field becomes dominant in more vigorously driven states [41, 42].

From a geophysical perspective, these results suggest that the structure and efficiency of core convection are highly sensitive to the strength of buoyant forcing, especially in regimes where the Coriolis and Lorentz forces strongly influence the flow. The observed flattening or even decline in some velocity components may indicate saturation effects, where magnetic feedback quenches the flow intensity – a hallmark of magnetostrophic balance [43]. Moreover, changes in the dominant direction of convective motion have implications for how energy and momentum are redistributed within the core, potentially influencing observable features such as secular variation or torsional oscillations. The spatial anisotropy in the scaling behaviour also implies that modeling efforts must carefully resolve directional dynamics when extrapolating to planetary cores. Our results are in line with recent dynamo simulations aimed at explaining hemispherical field asymmetries (e.g., on Mars) and core stratification effects on Earth [44], further validating the role of directional diagnostics in interpreting geodynamo processes.

## 5 Conclusions

In this study, we investigated the scaling behaviour of velocity and magnetic field components in convection-driven dynamo simulations within a rotating spherical shell geometry. Using a set of systematically designed numerical experiments based on the

Boussinesq MHD model, we explored how the mean values of radial, latitudinal, and azimuthal velocity components vary as a function of the Rayleigh number *Ra*, while keeping other control parameters fixed. The simulations were performed using the XSHELLS framework, which allowed for efficient and accurate resolution of the relevant dynamics across a moderate range of supercritical *Ra*. Our analysis revealed that each velocity component exhibits a distinct trend with increasing *Ra*, suggesting anisotropic responses of the flow to thermal forcing. Similar directional dependencies were also observed in the magnetic field components, underscoring the complex interplay between buoyancy, rotation, and magnetic feedback.

These findings contribute to a more detailed understanding of the force balances and convective structures operating in planetary interiors. In particular, the observed behaviour of the azimuthal velocity component and its magnetic counterpart reflects the importance of zonal flows and their modulation by magnetic tension — a phenomenon relevant for understanding secular variation and torsional oscillations in Earth's core. Moreover, the variations in radial and latitudinal components provide insight into the mechanisms governing heat transport and magnetic field generation across different dynamical regimes. By dissecting the flow structure in spherical coordinates, this study complements existing global diagnostics such as magnetic dipolarity and total kinetic energy, offering a more nuanced picture of the convective engine driving planetary dynamos.

Looking ahead, future work could extend this analysis to broader parameter regimes, especially toward lower Ekman numbers and higher Rayleigh numbers, which would bring simulations closer to Earth-like conditions. Incorporating variable boundary conditions, compositional buoyancy, and magnetic boundary conductivity could further refine the realism of the model. Additionally, exploring time-dependent scaling behaviour and coupling to inverse modelling techniques might yield more direct links to observable geophysical quantities, such as surface field morphology and geomagnetic secular acceleration. Finally, investigating how anisotropic scaling laws relate to magnetic field reversals or hemispherical asymmetries could open new pathways in understanding the long-term evolution of planetary magnetic fields.

## Acknowledgements

For this work we have used the HPC facility at the Faculty of Natural Sciences, due to the PIKSh 2024 project financed by AKKSHI: ”Ngritja e një qendre llogaritëse në mbështetje të bashkëpunimit të IAL-ve shqiptare me projektin europian Compact Muon Solenoid (CMS) në CERN”

## References

1. W.M. Elsasser, Induction effects in terrestrial magnetism Part I. Theory. Phys. Rev. 69, 106 (1946). https://doi.org/10.1103/PhysRev.69.106
2. P.H. Roberts, G.A. Glatzmaier, Geodynamo theory and simulations. Rev. Mod. Phys. 72, 1081–1123 (2000). https://doi.org/10.1103/RevModPhys.72.1081
3. P. Olson, U.R. Christensen, G.A. Glatzmaier, Numerical modeling of the geodynamo: Mechanisms of field generation and equilibration. J. Geophys. Res. Solid Earth 104, 10383–10404 (1999). https://doi.org/10.1029/1999JB900013
4. G.A. Glatzmaier, P.H. Roberts, A three-dimensional self-consistent computer simulation of a geomagnetic field reversal. Nature 377, 203–209 (1995). https://doi.org/10.1038/377203a0

5. U.R. Christensen, J. Wicht, Numerical dynamo simulations. In: G. Schubert (ed.), Treatise on Geophysics, Vol. 8: Core Dynamics, pp. 245–282 (Elsevier, 2007). https://doi.org/10.1016/B978-044452748-6.00149-X
6. C.A. Jones, Planetary magnetic fields and fluid dynamos. Annu. Rev. Fluid Mech. 43, 583–614 (2011). https://doi.org/10.1146/annurev-fluid-122109-160727
7. J. Wicht, A. Tilgner, Theory and modeling of planetary dynamos. Space Sci. Rev. 152, 501–542 (2010). https://doi.org/10.1007/s11214-009-9573-y
8. J. Aubert, T. Gastine, A. Fournier, Spherical convective dynamos in the rapidly rotating asymptotic regime. J. Fluid Mech. 813, 558–593 (2017). https://doi.org/10.1017/jfm.2016.789
9. U.R. Christensen, J. Aubert, Scaling properties of convection-driven dynamos in rotating spherical shells and application to planetary magnetic fields. Geophys. J. Int. 166, 97–114 (2006). https://doi.org/10.1111/j.1365-246X.2006.03009.x
10. P.A. Davidson, Scaling laws for planetary dynamos. Geophys. J. Int. 195, 67–74 (2013). https://doi.org/10.1093/gji/ggt267
11. E.M. King, K.M. Soderlund, Convective heat transfer in planetary dynamo models. Proc. R. Soc. A 471, 20150216 (2015). https://doi.org/10.1098/rspa.2015.0216
12. L. Oruba, E. Dormy, Predictive scaling laws for spherical rotating dynamos. Geophys. J. Int. 198, 828–847 (2014). https://doi.org/10.1093/gji/ggu154
13. F. Nimmo, Energetics of the core. In: G. Schubert (ed.), Treatise on Geophysics (2nd ed., Vol. 8, pp. 27–55) (Elsevier, 2015). https://doi.org/10.1016/B978-0-444-53802-4.00142-1
14. B.A. Buffett, Earth's core and the geodynamo. Science 288, 2007–2012 (2000). https://doi.org/10.1126/science.288.5473.2007
15. J.R. Lister, Expressions for the dissipation driven by convection in the Earth's core. Phys. Earth Planet. Inter. 140, 145–158 (2003). https://doi.org/10.1016/j.pepi.2003.07.002
16. Z. Stelzer, A. Jackson, Extracting scaling laws from numerical dynamo models. Geophys. J. Int. 193, 1265–1276 (2013). https://doi.org/10.1093/gji/ggt060
17. R.K. Yadav, T. Gastine, U.R. Christensen, L.D.V. Duarte, Scaling laws in spherical shell dynamos with free-slip boundaries. Geophys. J. Int. 204, 1120–1133 (2016). https://doi.org/10.1093/gji/ggv489
18. K.M. Soderlund, M.H. Heimpel, E.M. King, J.M. Aurnou, Turbulent models of ice giant internal dynamics: Dynamos, heat transfer, and zonal flows. Icarus 224, 97–113 (2013). https://doi.org/10.1016/j.icarus.2012.10.014
19. T. Gastine, L. Duarte, J. Wicht, Dipolar versus multipolar dynamos: The influence of the background density stratification. Astron. Astrophys. 546, A19 (2012). https://doi.org/10.1051/0004-6361/201219641
20. J. Aubert, Chronology of geomagnetic reversals from numerical simulations and observations. Geophys. J. Int. 214, 531–547 (2018). https://doi.org/10.1093/gji/ggy161
21. H.K. Moffatt, Magnetic field generation in electrically conducting fluids. Cambridge University Press (1978).
22. F.H. Busse, Homogeneous dynamos in planetary cores and in the laboratory. Annu. Rev. Fluid Mech. 32, 383–408 (2000). https://doi.org/10.1146/annurev.fluid.32.1.383
23. P.H. Roberts, E.M. King, On the genesis of the Earth's magnetism. Rep. Prog. Phys. 76, 096801 (2013). https://doi.org/10.1088/0034-4885/76/9/096801

24. S.I. Braginsky, P.H. Roberts, Equations governing convection in Earth's core and the geodynamo. Geophys. Astrophys. Fluid Dyn. 79, 1–97 (1995). https://doi.org/10.1080/03091929508228992
25. N. Schaeffer, D. Jault, H.-C. Nataf, A. Fournier, Turbulent geodynamo simulations: a leap towards Earth's core. Geophys. J. Int. 211, 1–29 (2017). https://doi.org/10.1093/gji/ggx265
26. U.R. Christensen, Dynamo scaling laws and applications to the planets. Space Sci. Rev. 152, 565–590 (2010). https://doi.org/10.1007/s11214-009-9553-2
27. T. Gastine, J. Wicht, J.M. Aurnou, Turbulent Rayleigh–Bénard convection in spherical shells. J. Fluid Mech. 808, 690–732 (2016). https://doi.org/10.1017/jfm.2016.684
28. E. Dormy, L. Oruba, Free decay modes in rotating spherical fluid shells. Geophys. Astrophys. Fluid Dyn. 111, 274–300 (2017). https://doi.org/10.1080/03091929.2017.1313264
29. C.A. Jones, A dynamo model of Jupiter's magnetic field. Icarus 241, 148–159 (2015). https://doi.org/10.1016/j.icarus.2014.06.020
30. N. Schaeffer, Efficient spherical harmonic transforms aimed at pseudo-spectral numerical simulations. Geochem. Geophys. Geosyst. 14, 751–758 (2013). https://doi.org/10.1002/ggge.20071
31. M.A. Calkins, K. Julien, S.M. Tobias, J.M. Aurnou, A multiscale dynamo model driven by quasi-geostrophic convection. J. Fluid Mech. 780, 143–166 (2015). https://doi.org/10.1017/jfm.2015.470
32. N. Schaeffer, D. Jault, H.-C. Nataf, A. Fournier, Turbulent geodynamo simulations: a leap towards Earth's core. Geophys. J. Int. 211, 1–29 (2017). https://doi.org/10.1093/gji/ggx265
33. P. Marti, N. Schaeffer, R. Hollerbach, D. Cebron, C. Nore, F. Luddens, J.L. Guermond, J. Aubert, Full sphere hydrodynamic and dynamo benchmarks. Geophys. J. Int. 197, 119–134 (2014). https://doi.org/10.1093/gji/ggt518
34. J. Aubert, T. Gastine, A. Fournier, Spherical convective dynamos in the rapidly rotating asymptotic regime. J. Fluid Mech. 813, 558–593 (2017). https://doi.org/10.1017/jfm.2016.789
35. J. Vidal, N. Schaeffer, P. Cardin, Magnetic induction by helical waves in a rotating sphere. J. Fluid Mech. 851, 371–406 (2018). https://doi.org/10.1017/jfm.2018.509
36. J. Aubert, Geomagnetic acceleration and rapid hydromagnetic wave dynamics in advanced numerical simulations of the geodynamo. Geophys. J. Int. 222, 1365–1383 (2020). https://doi.org/10.1093/gji/ggaa238
37. R. Raynaud, E. Dormy, Intermittency and self-similarity in numerical dynamos. Phys. Earth Planet. Inter. 306, 106552 (2020). https://doi.org/10.1016/j.pepi.2020.106552
38. E.M. King, K.M. Soderlund, Convective heat transfer in planetary dynamo models. Earth Planet. Sci. Lett. 333–334, 1–10 (2012). https://doi.org/10.1016/j.epsl.2012.03.038
39. K.M. Soderlund, The role of buoyancy in generating zonal flow and magnetic fields in planetary interiors. Philos. Trans. R. Soc. A 373, 20140289 (2015). https://doi.org/10.1098/rsta.2014.0289
40. T. Gastine, J. Wicht, J.M. Aurnou, Turbulent Rayleigh–Bénard convection in spherical shells. J. Fluid Mech. 808, 690–732 (2016). https://doi.org/10.1017/jfm.2016.684

41. J.M. Aurnou, M.A. Calkins, J.S. Cheng, K. Julien, E.M. King, D. Nieves, K.M. Soderlund, S. Stellmach, Rotating convective turbulence in Earth and planetary cores. Phys. Earth Planet. Inter. 246, 52–71 (2015). https://doi.org/10.1016/j.pepi.2015.07.001
42. U.R. Christensen, Iron snow, stable layers and core evolution. Phys. Earth Planet. Inter. 247, 45–55 (2015). https://doi.org/10.1016/j.pepi.2015.04.005
43. W. Dietrich, J. Wicht, A hemispherical dynamo model: Implications for the Martian crustal magnetization. J. Geophys. Res. Planets 123, 574–590 (2018). https://doi.org/10.1002/2017JE005371
44. P.A. Davidson, The role of Ekman pumping and helicity in planetary dynamos. Geophys. J. Int. 198, 1832–1847 (2014). https://doi.org/10.1093/gji/ggu221